Thief Zone Identification through Seismic Monitoring of a CO_2 Flood, Weyburn Field, Saskatchewan

A. W. Araman, M. Hoffman and T. L. Davis

PROFESSIONAL PAPER

Located in the Williston Basin (Figure 1) in Southeastern Saskatchewan, Weyburn Field implemented eight years ago a CO_2 EOR project in order to maximize recovery from the fields main producing unit: a carbonate reservoir known as the Midale Beds. To date, Weyburn Field has produced 335 million barrels of oil and has an estimated 1.4 billion barrels OOIP.[5] This paper demonstrates that Time-Lapse and Multi component seismic data analysis is an effective tool for monitoring CO_2 injection through the detection of changes in reservoir properties such as porosity, fluid distribution, and fracture density. The monitoring of these changes directly informs the design of the EOR project, thus optimizing field recovery. Evaluation of P-wave Time-Lapse and S-wave data resulted in the following conclusions regarding production in Weyburn field:
1. The Midale reservoir is experiencing a downward loss in CO_2 in the west corner of the study area. Shifting the location of the nearby injection well is recommended.
2. Throughout the field, P-wave time-lapse shows that CO_2 is largely confined to NW-SE fracture orientation identified after interpretation of the 2000 S-wave data.

Key words: CO_2 flood, EOR strategy, multicomponent seismic analysis, seismic monitoring, time-lapse analysis

Introduction

Limited subsurface data and detailed reservoir characterization make the initial design of EOR projects problematic. Unexpected reservoir heterogeneities influence the spatial distribution of water floods and CO_2 injections. Monitoring both the temporal and spatial variability of an EOR project is necessary to inform adjustments in the placement of injecting and producing wells in order to optimize recovery. The use of Time-Lapse and Multi component seismic to monitor an EOR project at Weyburn Field has proven to be an effective method for monitoring changes in the physical characteristics of the reservoir and the distribution of a CO_2 flood.

The main producing unit at Weyburn Field is the Midale Reservoir of the Mississippian Charles Formation (Figure 2). The Midale Beds exist at depths ranging from 1300 to 1500 meters and are subdivided into an upper Marly zone and a lower Vuggy zone. Currently, Weyburn Field has produced 335 million barrels of oil with an estimated 1.4 billion barrels OOIP[5] (Figure 3)

The goal of this paper is to analyze the sweep efficiency of the EOR plan at Weyburn Field using 3-D P-wave Time-Lapse and Multi component seismic data.

History of Production at Weyburn Field

Weyburn Field was discovered in 1954 and produced on primary production for nearly 10 years. In 1964 a water

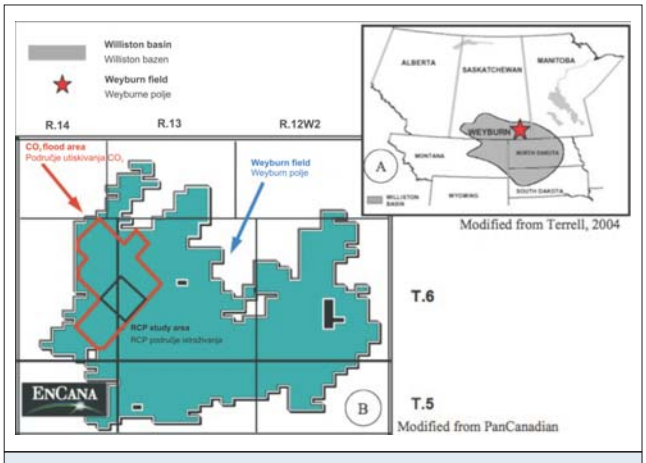

Fig. 1. Location map of Weyburn Field[14]
Sl. 1. Lokacija Weyburn polja[14]

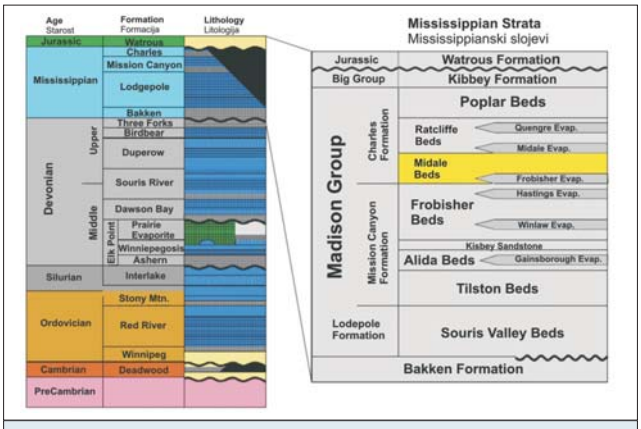

Fig. 2. Stratigraphic column showing the location of the Midale Bed[14]
Sl. 2. Stratigrafski presjek Midale slojeva[14]

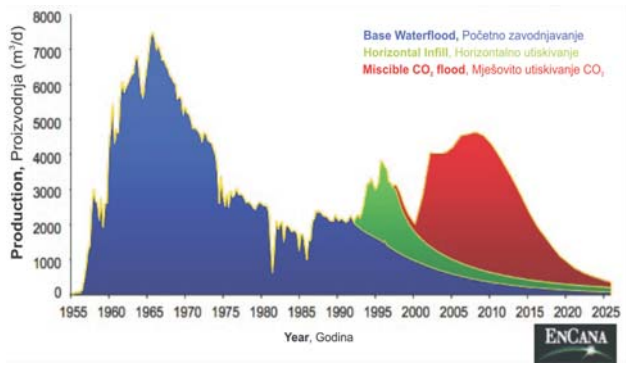

Fig. 3. Oil production history[5]
Sl. 3. Povijest proizvodnje nafte[5]

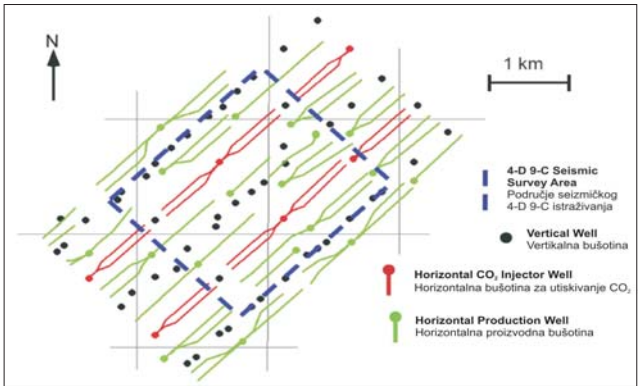

Fig. 4. CO_2 injection pattern[5]
Sl. 4. Shema utiskivanja CO_2[5]

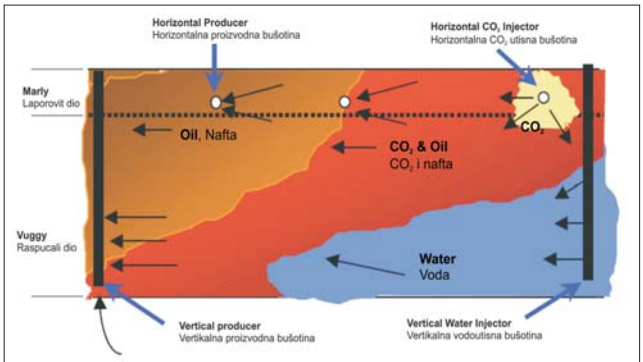

Fig. 5. EOR strategy for the Weyburn Field[14]
Sl. 5. EOR strategija za Weyburn polje[14]

flood was implemented and peak production was reached for the field in 1965 at 46.000 barrels/day (Figure 3). The water flood preferentially swept the upper Vuggy unit due to its fractured nature, bypassing oil within the lower Marly unit. In 1991, horizontal in filling began to target oil in the Marly that was unaffected by the previous water floods.[5]

In 2000, an EOR program was implemented by ENCANA (Figure 4) that consisted of Simultaneous, but Separate Water and CO_2 Injection (SSWG) (Figure 5).

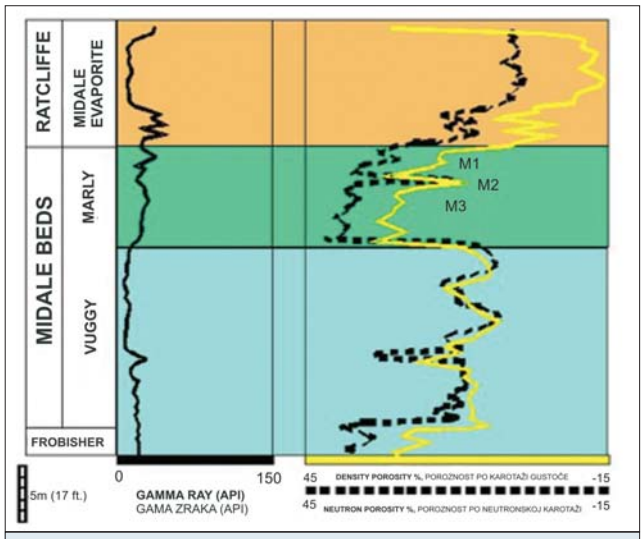

Fig. 6. Gamma Ray, Density Porosity and Neutron Porosity logs[12]
Sl. 6. Karotažni gamma, density i neutron porosity dijagrami

This project is estimated to prolong the field life by 20 years with an added 30% barrels of incremental oil recovery.[5]

Seismic Monitoring for EOR

This study utilizes a 3-D baseline survey taken in 2000 and a second 3-D monitoring survey acquired in 2002 for P-wave Time-Lapse analysis. Through the examination of RMS amplitude differences between the 2000 and 2002 surveys, we are able to detect spatial distribution of the CO_2 flood.[7]

This study also utilizes S-wave data acquired in 2000 to characterize velocity anisotropies within the Midale Reservoir. These velocity anisotropies are detected through differences in S_1 and S_2 velocities and are attributed to fracture trends within the reservoir.

Field Geology

The main producing unit in the field are the Midale Beds of the Mississippian Charles Formation. The Midale Beds exist at depths that range from 1300 to 1500 meters. The Midale Beds consist of three subunits: (1) the Frobisher, (2) the Midale Vuggy, and (3) the Midale Marly. These units can be characterized as a shallowing upward carbonate sequence formed in an arid tidal flat ramp depositional environment.

Deposition of the Midale Beds occurred as a result of a westward shift of an intra-cratonic seaway, leading to shallowing in the study area. Following the shift, subsidence occurred on the ramp and deposition of ramp carbonates (Midale Beds) commenced.[12] The Midale Marly, an intertidal/lagoonal facies, is a dolostone of mudstone to wackestone in texture. The Marly has an average porosity of 26% (range of 20-37%) with an average permeability of 10 md (range of 0.1-150 md).[14] (Figure 6)

The Midale Vuggy can be subdivided into shoal and intershoal facies. The Vuggy shoal is characterized as a packstone to grainstone with an average porosity of 15% (range of 10-21%) with an average permeability of 50 md (range of 1-500 md). The Vuggy intershoal is character-

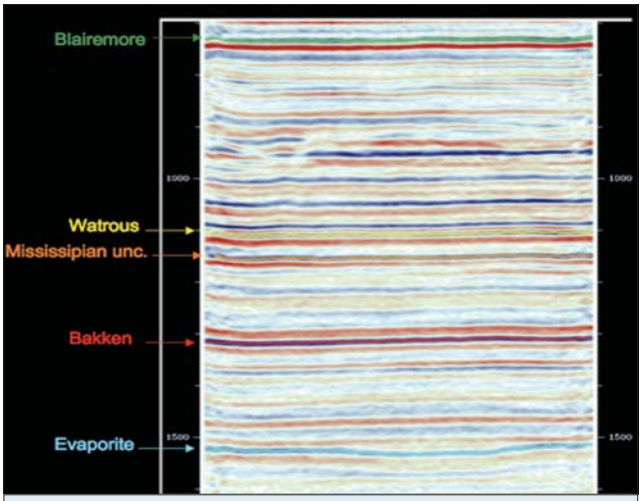

Fig. 7. Line 67 from the 2000 3-D survey with the 5 horizons of interest shown on the this specific 2-D line
Sl. 7. Profil 67 iz 3-D snimanja 2000. godine s označenih 5 zanimljivih horizonata

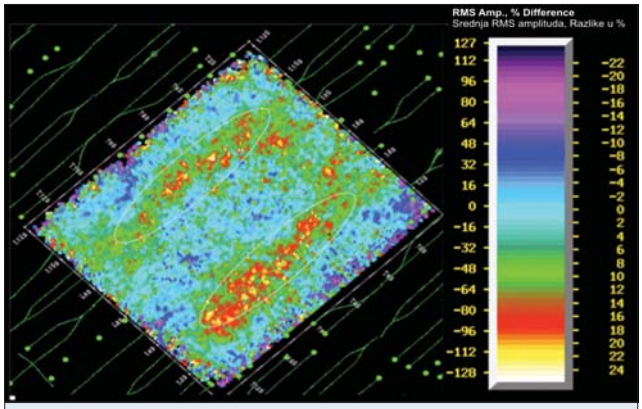

Fig. 8. Time-Lapse over the 7-12 ms interval below the Mississippian unconformity
Sl. 8. Promjena amplitude u intervalu od 7-12 ms ispod mississippianske diskordancije

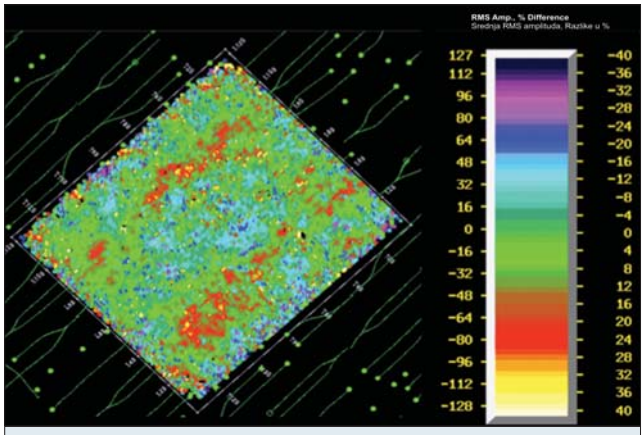

Fig. 9. Time-Lapse over the 5-7 ms interval below the Mississippian unconformity
Sl. 9. Promjena amplitude u intervalu od 5-7 ms ispod mississippianske diskordancije

ized as a mudstone to packs tone with an average porosity of 10% (range of 2-15%) with an average permeability of 3 md (range of 0.01-20 md).[14] (Figure 6)

The source rock for the Midale Beds is the underlying Shale. Oil was generated in the Bakken within the Williston Basin near the Nessen anticline, with peak generation occurring in the Cretaceous.[12] Reservoir traps are nearly entirely stratigraphic, dominated by the updip pinch out of permeability and porosity related to the overlying Mississippian unconformity. Local facies changes and stratigraphic seals immediately underlying the unconformity may also serve as trapping mechanisms.[12]

Time-Lapse Analysis of the Midale Beds

Five main horizons have been picked on the 2000 and 2002 P-wave data.[4] These five horizons displayed on the 2000 P-wave data are shown in Figure 7. We are particularly interested in the Mississippian unconformity and the Bakken horizon because they define the two reservoirs we want to characterize. The compressional wave seismic is shown in Figure 7. The reflectors are flat, the bandwidth frequency is high (up to 150 Hz were recovered on the high end), and there are no major structural events.

RMS amplitude maps have been generated for different intervals below the Mississippian unconformity, the goal being to characterize the CO_2 flow in the survey area. The presence of CO_2 in the formation changes the properties of the rocks. CO_2 has unique properties: it is a very dense and very compressible fluid. Its presence is detected by the variation of the seismic amplitude response before and after CO_2 injection. Time-Lapse maps showing the evolution of the P-wave *RMS* amplitude between 2000 and 2002 as a percentage of the 2000 *RMS* amplitude have been generated using Equation 1.[17]

$$Time-Lapse = \frac{RMS_{p-wave}2002 - RMS_{pwave}2000}{RMS_{pwave}2000} \quad (1)$$

Figure 8 shows a difference on the order of 14% along the injection wells at a 5 ms time window below the Mississippian unconformity. The CO_2 did flow in the Midale Beds and the direction of its flow is parallel to the injection well. We can also notice that the flow along the southern well is more pronounced that the northern one.

The following step is to break the Midale into 2 ms intervals (it is the smallest resolution supported by the quality of our picked horizons) in order to monitor the depth of diffusion of the CO_2 in the formation. Figures 9 to 13 show that the CO_2 is present in the Midale beds up to 13 ms below the Mississippian unconformity. The CO_2 did propagate along the injection wells. This is a proof of a high permeability matrix in the Midale Beds having a SW-NE orientation.

Figure 13 shows the transition zone where the CO_2 seems to be present throughout in the formation. This corresponds to the interval between 13 and 15 ms below the Mississippian unconformity. The *RMS* amplitude difference is important in many areas and there seems to be no defined trend. Just below this area, the *RMS* amplitude difference drops to zero. No CO_2 is present in this area. This corresponds to the Frobisher Evaporites (Figure 3). The Frobisher Beds are quite thick in time, and the *RMS* amplitude difference remains null on a 30 ms

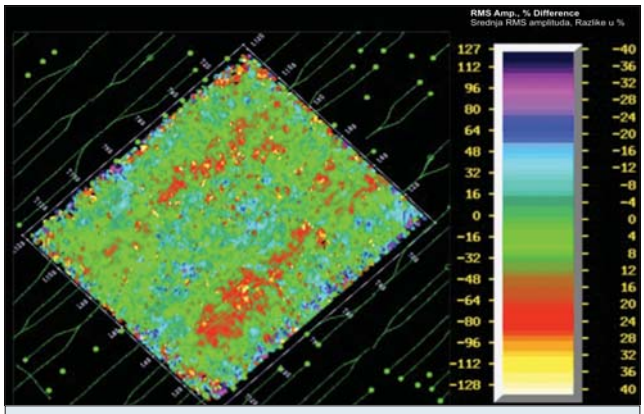

Fig. 10. Time-Lapse over the 7-9 ms interval below the Mississippian unconformity
Sl. 10. Promjena amplitude u intervalu od 7-9 ms ispod mississippianske diskordancije

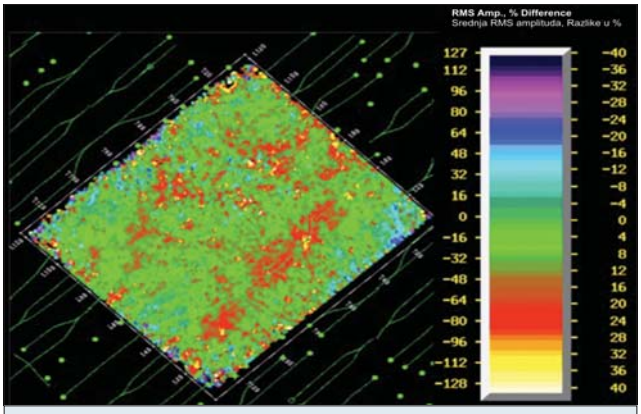

Fig. 12. Time-Lapse over the 11-13 ms interval below the Mississippian unconformity
Sl. 12. Promjena amplitude u intervalu od 11-13 ms ispod mississippianske diskordancije

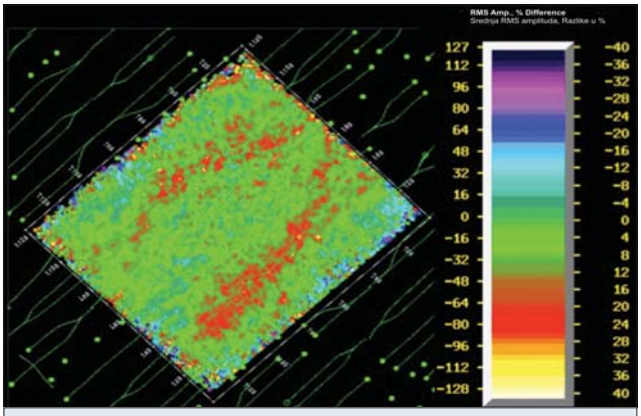

Fig. 11. Time-Lapse over the 9-11 ms interval below the Mississippian unconformity
Sl. 11. Promjena amplitude u intervalu od 9-11 ms ispod mississippianske diskordancije

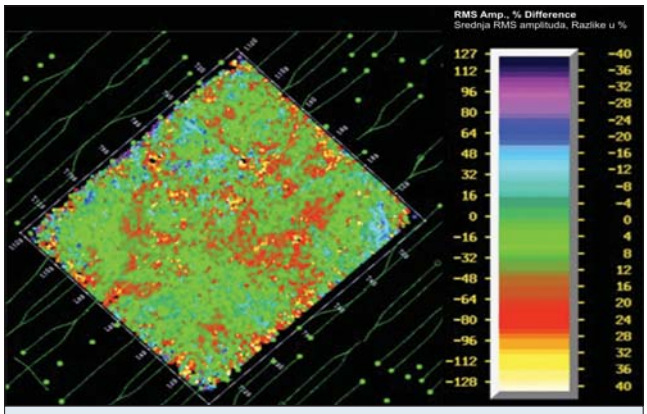

Fig. 13. Time-Lapse over the 13-15 ms interval below the Mississippian unconformity
Sl. 13. Promjena amplitude u intervalu od 13-15 ms ispod mississippianske diskordancije

interval. The *RMS* amplitude difference remains equal to zero from 15 ms to 45 ms below the Mississippian unconformity. Figures 14, 15 and 16 show three 3 ms intervals where the RMS amplitude difference is zero. The common wisdom would have been to state that the CO_2 did not flow deeper in the formation because it was sealed by the Frobisher Formation.

Figure 16 proved the contrary: we see a 20% *RMS* amplitude difference located in three areas along the injection wells: one big area where CO_2 seems to be confined in the western part of the northern well and two small areas along the southern well. One of the main questions is how that CO_2 escaped form the Midale reservoir and has been confined in a small 5 ms interval, 30 ms below the Midale Beds?

In order to answer to that question, we have examined carefully the *RMS* amplitude map of the Vuggy zone extracted from the 2000 P-wave data (Figure 17). The Vuggy zone seems to be characterized by medium to low amplitudes except on the northwestern part of the survey area where very high amplitudes are present. In fact those high amplitudes are related to shoals and the very low amplitudes to evaporite. Hence, the CO_2 could not have escaped where the evaporite is present, and did only escape though the shoals fractures to the northwest. This is the only part where shoals are present in important proportions and this is where the CO_2 escaped. This small 5 ms interval where the CO_2 is conned is probably the Kisbey Sandstone (Figure 2) sealed upward by the Winlaw Evaporite of the Frobisher Beds and downward by the Gainsborough Evaporite of the Alida Beds. Figure 18 is a comparison of the *RMS* amplitude map of the Vuggy formation of the Midale reservoir and the Time-Lapse map for the 45-50 ms interval below the Mississippian unconformity corresponding to the Kisbey Sandstone where the CO_2 has escaped through the shoals fracture. The two maps match well and prove the theory of the CO_2 escaping downward through fractures.

Figure 19 is a Time-Lapse analysis on the Ratcliffe Beds above the Midale Reservoir. The *RMS* amplitude difference is null. No CO_2 is found in this formation: the Ratcliffe Beds form an effective seal to the Midale Reservoir.

Multi component Seismic Analysis of the Midale Reservoir

After having monitored the CO_2 flow, our next step is to characterize the fracture orientation in the reservoir. To

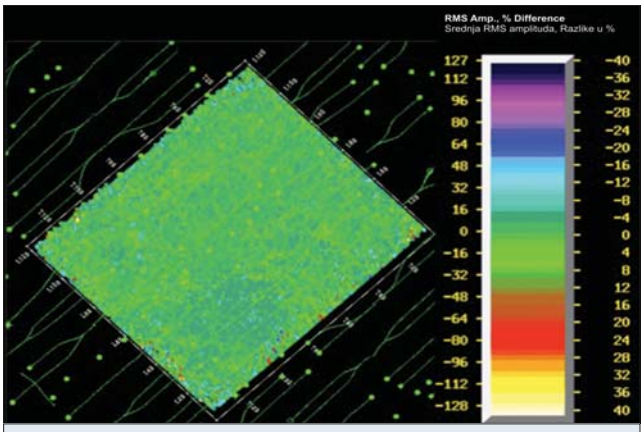

Fig. 14. Time-Lapse over the 15-17 ms interval below the Mississippian unconformity. The RMS amplitude difference is equal to zero. CO_2 did not infiltrate this interval.
Sl. 14. Promjena amplitude u intervalu od 15-17 ms ispod mississippianske diskordancije. Srednja (RMS) razlika amplituda jednaka je nuli. Znači da CO_2 nije prodro u taj interval.

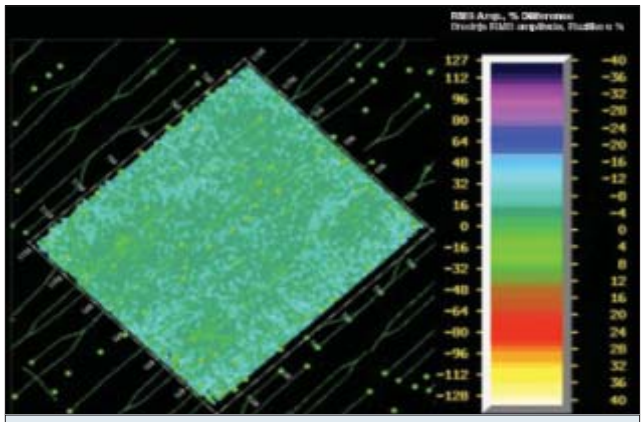

Fig. 15. Time-Lapse over the 25-30 ms interval below the Mississippian unconformity
Sl. 15. Promjena amplitude u intervalu od 25-30 ms ispod mississippianske diskordancije

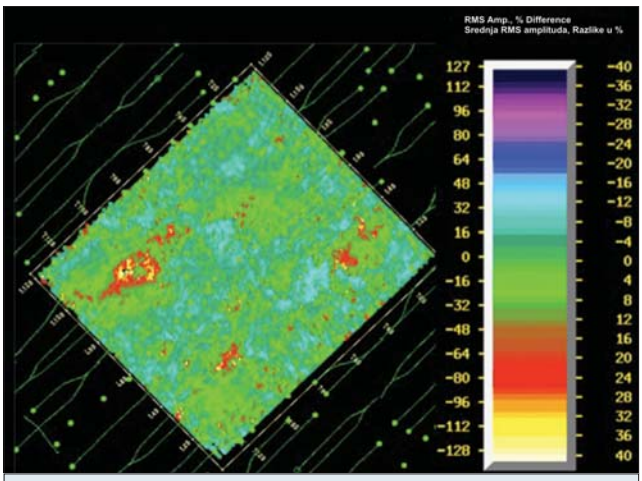

Fig. 16. Time-Lapse over the 45-50 ms interval below the Mississippian unconformity. The RMS amplitude difference is not equal to zero everywhere. CO_2 migrated downward from the Midale interval to the Kisbey Sandstone
Sl. 16. Promjena amplitude u intervalu od 45-50 ms ispod mississippianske diskordancije. Srednja (RMS) razlika amplituda na cijelom je području različita od nule. Znači da je CO_2 migrirao prema dolje iz Midale intervala do Kisbey pješčenjaka.

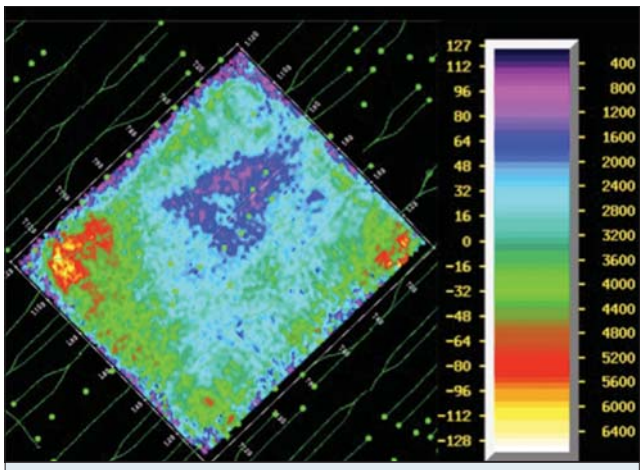

Fig. 17. RMS amplitude on the 7-12 ms below the Mississippian unconformity in the Midale Reservoir High amplitude represent shoals while low amplitude represent evaporite
Sl. 17. Srednja (RMS) amplituda na intervalu 7-12 ms ispod mississippianske diskordancije u Midale ležištu. Velike vrijednosti amplituda odgovaraju priobalnim sedimentima, a male evaporitima.

achieve this goal, we will study the anisotropy computed from the shear wave data shot in 2000.[2] anisotropy can be characterized as the time between the S_1 and the S_2 waves.[2] In fact, if the formation was ideally isotropic, there would not be any time between the shear wave propagating horizontally in the formation according to two perpendicular directions. On the other hand, if the formation is anisotropic, there would be a difference between the propagation time in the two orthogonal directions. The percentage of propagation time difference is a concrete measure of the anisotropy.[3]

Figure 20 shows the S_1 and the S_2 wave as recorded from the 2000 survey. We are interested in two horizons: the Shaunavon horizon which is located 270 ms above the Midale reservoir and which lights up nicely on the shear seismic gather and the Bakken horizon. Our first step will be to use these two horizons to try to find a general anisotropy trend for the whole formation. This is done by subtracting the time difference between the Bakken and the Shaunavon horizons in S_1 from S_2 and by normalizing it by the time difference between these two horizons for S_2. Equation 2 is the general equation used for the computation of the anisotropy shown in Figure 21. The practical computation is made using Equation 3.

$$\%\,Anisotropy = 100 \times \frac{\Delta t_{s1} - \Delta t_{s2}}{\Delta t_{s2}} \qquad (2)$$

$$\%\,Anisotropy = 100 \times \frac{(B_{S1} - S_{S1}) - (B_{S2} - S_{S2})}{(B_{S2} - S_{S2})} \qquad (3)$$

Where:

B_{S1} is the Bakken horizon on S_1 shear wave

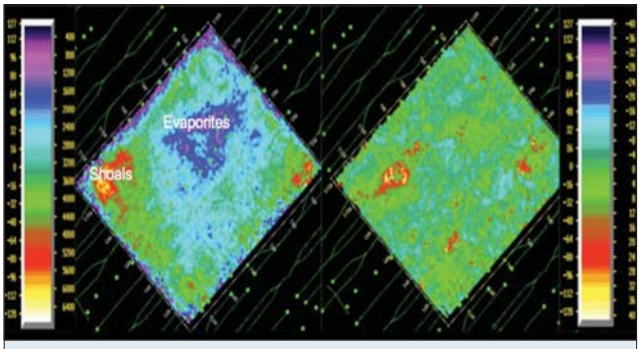

Fig. 18. Comparison between the Midale RMS amplitude map and the Time-Lapse map
Sl. 18. Usporedba karti srednje (RMS) amplitude i karte promjena amplitude u Midale ležištu

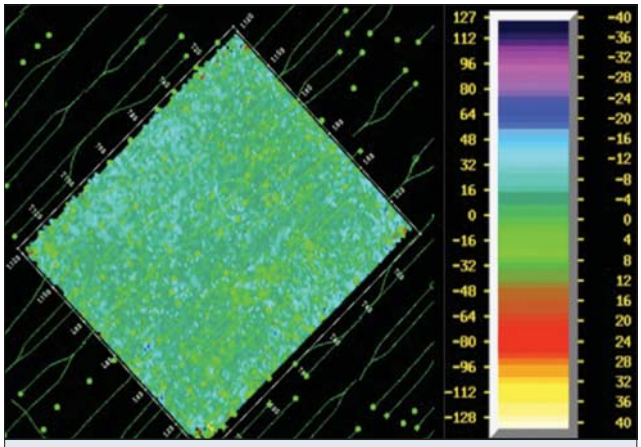

Fig. 19. Time-lapse on the Beds above the Midale Reservoir
Sl. 19. Karta promjena amplituda u Ratcliffe slojevima u krovini Midale ležišta

B_{S2} is the Bakken horizon on S_2 shear wave

S_{S1} is the Shaunavon horizon on S_1 shear wave

S_{S2} is the Shaunavon horizon on S_2 shear wave

The very high amplitude differences seen on the edges of the map are due to edge effects. The shear wave data being very noisy, specially on the edges of the survey, an accurate horizon picking in these areas is very hard to achieve. It seems that there are two sets of anisotropy orientation in the whole Shaunavon-Bakken section: one set has a SW-NE direction and is parallel to the injection wells and another set seems to have a SE-NW direction and is perpendicular to the injection wells. The anisotropy is as high as 3.5% in some areas on the whole section. The anisotropy is directly related to the fractures. We have hence two general sets of fractures oriented perpendicularly. The set of fractures perpendicular to the injection wells explains what has been seen on Time-Lapse maps: the CO_2 moving along the injection wells.

Another computation of the anisotropy is based on the RMS amplitude between S_1 and S_2. This technique gives us a better understanding of the anisotropy in the Midale reservoir. Equation 4 shows how the anisotropy is computed and Figure 23 shows the result of our computation.

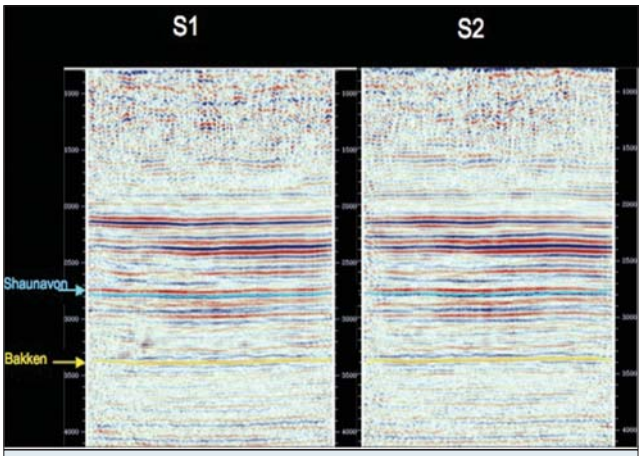

Fig. 20. S_1 and S_2 shear waves for the Line 67 of the 2000 3D multi component seismic survey
Sl. 20. Snimke S_1 i S_2 transverzalnih valova na profilu 67 snimljenom 3D višekomponentnih seizmičkih snimanja tijekom

$$\%\,Anisotropy = 100 \times \frac{RMS_{S1} - RMS_{S2}}{RMS_{S2}} \quad (4)$$

Where:

RMS_{S1} is the *RMS* amplitude computed on S_1 shear wave data in the reservoir interval (between 270 and 320 ms below the Shaunavon horizon).

RMS_{S2} is the *RMS* amplitude computed on S_2 shear wave data in the reservoir interval (between 270 and 320 ms below the Shaunavon horizon).

From Figure 22 it is clear that there is a general anisotropy trend, and hence a general set of fractures having a SW-NE orientation parallel to the injection wells. This is concordant with the CO_2 movement along the injection wells. The amplitudes obtained using Equation 4 are too high. Therefore, we used a calculation of the general percentage of anisotropy difference (Equation 5) which gives more realistic values for the anisotropy.

$$\%\,Anisotropy = 100 \times \frac{RMS_{S1} - RMS_{S2}}{\frac{1}{2} \times (RMS_{S2} + RMS_{S2})} \quad (5)$$

The results based on Equation 5 are shown in Figure 23. The general orientation of fractures parallel to the injection well is enhanced by important anisotropy values that reach 30% in some thin areas parallel to the injection wells. The CO_2 used these fractures to migrate along the wells. Unfortunately as we have seen in the previous section, the CO_2 did not stay where we initially planned for it to stay, which is in the Midale formation, in order to enhance the hydrocarbon recovery, but did escape to a lower formation. The position of some of the injection wells should be reconsidered but certainly not their direction which is optimal for the CO_2 flooding.

Conclusion

Time-Lapse monitoring showed that the CO_2 injected moved along the injection wells in the Midale reservoir. Shear wave analysis showed that the fracture trend in the Midale was parallel to the injection wells, which explained the movement of the CO_2 in that same direction.

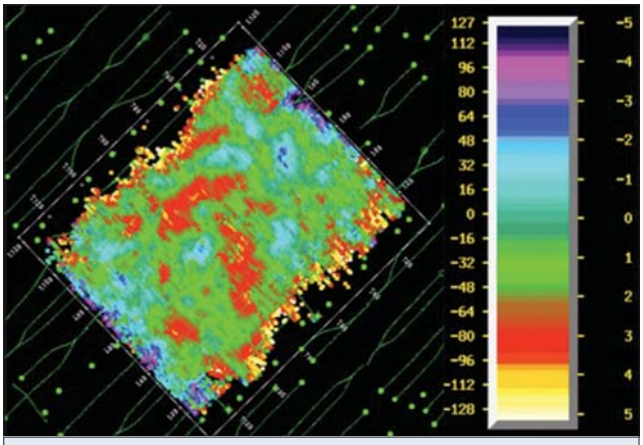

Fig. 21. Percentage anisotropy difference based on isochrone between the Bakken and the Shaunavon formations
Sl. 21. Postotak razlike anizotropičnosti određen na temelju razlika izokrona među Bakken i Shaunavon formacija

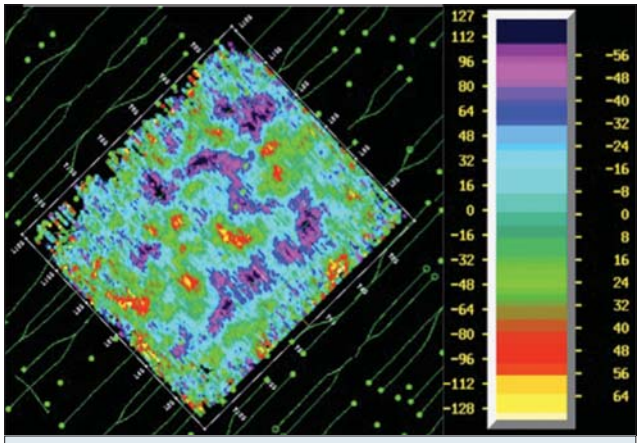

Fig. 23. Percentage RMS difference normalized by the shear waves mean between S_1 and S_2 in the Midale reservoir
Sl. 23. Postotak srednje (RMS) razlike među S_1 i S_2 valovima normaliziran sa srednjom vrijednošću transverzalnih valova u Midale ležištu

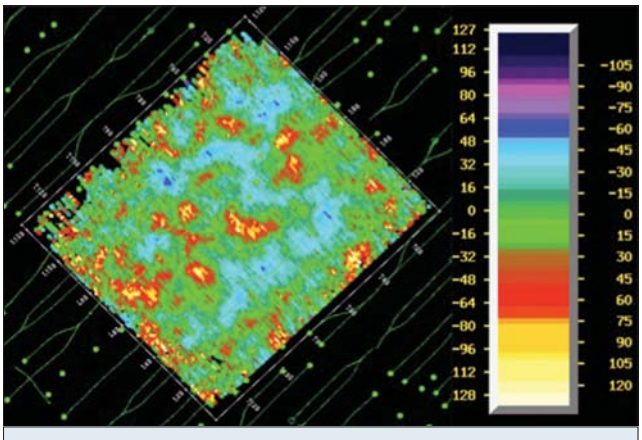

Fig. 22. Percentage RMS difference between S_1 and S_2 in the Midale reservoir
Sl. 22. Postotak srednje (RMS) razlike među S_1 i S_2 valovima u Midale ležištu

Further investigation and time splitting of the intervals below the Midale Beds followed by Time-Lapse analysis showed that the CO_2 escaped downward from the Midale Beds through fractures in the shoals and was trapped in the Kisbey Sandstone sealed upward by the Winlaw Evaporite of the Frobisher Beds and downward by the Gainsborough Evaporite of the Alida Beds. The direction of the injection wells is ideal (parallel to the fracture set), but the location of the wells has to be chosen more carefully in order to avoid CO_2 losses.

References

1. K. C. Bard, J. F. Arestad, A. Al-Bastaki, T. L. Davis, and R. D. Benson. Integrated reservoir characterization of a complex carbonate field. *Society of Petroleum Engineers*, October 1995.
2. G. Bellefleur, L. Adam, D. White, B. Mattocks, and T. L. Davis. Seismic imaging and anisotropy analysis of 9C data at Weybur Field, Saskatchewan, Canada. *73th Ann. Internat. Mtg. : Soc. of Expl. Geophys.*, 22(7):1350-1353, 2003.
3. R. D. Benson and T. L. Davis. Multi component seismic monitoring of a miscible CO_2 floor, Weybur Field, Canada. *65th Mtg: Eur. Assn. Geosci . Eng.*, pages 1673-1676, 2003.
4. R. Bunge. Midale reservoir fracture character using integrated well and seismic data, Weyburn Field, Saskatchewan. Master's thesis, Colorado School of Mines, 2000.
5. T. Davis and S. Roche. Time-Lapse, Multi component Seismology, Application to Dynamic Reservoir Characterization. *Colorado School of Mines, Department of Geophysics*, pages 157-187, 2006.
6. T. L. Davis and R. D. Benson. Weyburn Field monitoring project, seismic filtering. *Soc. of Exp. Geophys*., pages 2255-2258, 2004.
7. T. L. Davis, R. D. Benson, R. Cardona, R. R. Kendall, and R. Winarski. Multi component seismic characterization and monitoring of the CO_2 flood at Weyburn Field, Saskatchewan, Canada. *The Leading Edge*, 22(7):696-697, 2003.
8. B. DeVault, T. L. Davis, I. Tsvankin, and R. Verm. Multi component AVO analysis, Vacuum Field, New Mexico. *Geophysics*, 67(3):701-710, May-June 1995.
9. C. Lewis, T. L. Davis, and C. Vuillermoz. Three-dimensional multi component imaging of reservoir heterogeneity, Silo Field, Wyoming. *Geophysics*, 56(12):2048-2056, December, 1991.
10. M. A. Martin and T. L. Davis. Shear-wave birefringence; a new tool for evaluating fractured reservoirs. Geophysics: *The Leading Edge of Exploration*, 27, October 1987.
11. F. F. Meissner. Petroleum geology of the Bakken Formation Williston Basin, North Dakota and Montana. *Montana Geological Society 1978, Williston Basin Symposium*, pages 207-227, 1978.
12. N. Pendrigh. Facies control on CO_2 flooding of a thin carbonate reservoir,Weyburn Field, Saskatchewan. Master's thesis, Colorado School of Mines, 2005.
13. M. J. Pranter, N. F. Hurley, and T. L. Davis. Dual-lateral horizontal wells successfully target bypassed pay in the San Andreas Formation, Vacuum Field, New Mexico. *AAPG Bulletin*, 88(1):99-113, January 2004.
14. N. Royer. Time-Lapse P-Wave seismic monitoring of the CO_2 flood at Weyburn Field, Saskatchewan. Master's thesis, Colorado School of Mines, 2004.
15. E. L. Shuck, T. L. Davis, and R. D. Benson. Multi component 3-D characterization of coalbed methane reservoir. Geophysics, 61(2):315-330, March-April 1996.
16. M. Smith and R. Bustin. Late Devonian and Early Mississippian Bakken and Exshaw Black Shale source rocks, Western Canada Sedimentary Basin: A sequence stratigraphy interpretation. *AAPG Bulletin*, 84(7):940-960, 2000.
17. M. Terrell, T. L. Davis, L. Brown, and R. Fuck. Seismic monitoring of a CO_2 flood at Weyburn Field, Saskatchewan, Canada: Demonstrating the robustness of time-lapse seismology. *72th Ann. Internat. Mtg. : Soc. of Expl. Geophys.*, pages 1673-1676, 2002.

❖

Authors:

A. W. Araman, Colorado School of Mines, Department of Geophysic, Golden Colorado. e-mail: aaraman@mines.edu

M. Hoffman, Colorado School of Mines, Department of Geology, Golden Colorado. e-mail: mahoffma@mines.edu

T. L. Davis, Colorado School of Mines, Department of Geophysic, Golden Colorado. e-mail: tdavis@mines.edu